Inorg. Chem. **2003**, *42*, 6041–6049

Fluorinated Aminoalkoxide and Ketoiminate Indium Complexes as MOCVD Precursors for In_2O_3 Thin Film Deposition

Tsung-Yi Chou, Yun Chi,* Shu-Fen Huang, and Chao-Shiuan Liu

Department of Chemistry, National Tsing Hua University, Hsinchu 30013, Taiwan, Republic of China

Arthur J. Carty,* Ludmila Scoles, and Konstantin A. Udachin

Steacie Institute for Molecular Sciences, National Research Council Canada, 100 Sussex Drive, Ottawa, Ontario K1A 0R6, Canada

Received May 29, 2003

The syntheses of two distinctive types of indium complex derived from trimethylindium ($InMe_3$) are reported. The first kind has a generalized structural formula $[InMe_2(amak)]_2$, where (amak)H is an abbreviation for a series of chelating amino alcohol ligands $HOC(CF_3)_2CH_2NHR$, R = $(CH_2)_2OMe$ (**1**), Me (**2**), and Bu^t (**3**), as well as $HOC(CF_3)_2CH_2NMe_2$ (**4**); while the second type of complex is illustrated by $[InMe_2(keim)]$ (**5**), for which (keim)H is a tridentate ketoimine ligand of structural formula $O{=}C(CF_3)CH_2C(CF_3){=}NCH_2CH_2NMe_2$. The solid-state structures of **2** and **5** were determined using single crystal X-ray diffraction studies. For the aminoalkoxide complexes **2**–**4**, the existence of dimeric In_2O_2 core structures in the solid state has been established with the amino fragment located *trans* to the alkoxide ligands, in a molecular arrangement which is in contrast to the distorted, trigonal bipyramidal geometry observed for the ketoiminate complex **5**. Moreover, VT NMR studies of **2** revealed a rapid dimer-to-monomer equilibration and simultaneous rupture of the N→In dative interaction, affording two interconvertible isomers related by having the N–Me substituents in either *trans* or *cis* dispositions. For complexes **2** and **5**, deposition of In_2O_3 thin films was successfully conducted at temperatures 400–500 °C, using O_2 as the carrier gas to induce indium oxide deposition and to suppress carbon impurity present in the thin film. Scanning electron micrographs (SEMs) revealed the surface morphologies. The atomic composition of these films was examined by both X-ray photoelectron spectroscopy (XPS) and Rutherford backscattering (RBS) methods, while X-ray diffraction studies (XRD) confirmed the formation of a preferred orientation along the (222) planes.

In recent years, there has been increasing interest in the synthesis of new organoindium compounds because of their potential use as CVD precursors for the production of III−V and III−VI composite semiconductors.[1] Pioneering work was carried out by Cowley and Jones,[2] who synthesized complexes of general formula $(L_nInEL'_n)_x$, featuring the desired 1:1 stoichiometry between the indium atom and the group V elements E, E = N, P, or As. In these compounds, the ligands L and L′ can undergo facile dissociation upon thermal decomposition affording as deposited thin film materials with a 1:1 ratio of indium to pnictide element E. Through these and related studies, the concept of so-called single molecule precursors was developed.[3] Subsequently, CVD techniques using these source complexes have been greatly extended

* Authors to whom correspondence should be addressed. E-mail: ychi@mx.nthu.edu.tw (Y.C.). Fax: (886) 3 572-0864 (Y.C.); arthur.carty@nrc-cnrc.gc.ca (A.J.C.). Fax: (613) 957-8850.

(1) (a) Fischer, R. A.; Sussek, H.; Miehr, A.; Pritzkow, H.; Herdtweck, E. *J. Organomet. Chem.* **1997**, *548*, 73. (b) Neumayer, D. A.; Cowley, A. H.; Decken, A.; Jones, R. A.; Lakhotia, V.; Ekerdt, J. G. *J. Am. Chem. Soc.* **1995**, *117*, 5893. (c) Kim, J.; Bott, S. G.; Hoffman, D. M. *J. Chem. Soc., Dalton Trans.* **1999**, 141. (d) Suh, S.; Hoffman, D. M. *J. Am. Chem. Soc.* **2000**, *122*, 9396. (e) Lobinger, P.; Park, H. S.; Hohmeister, H.; Roesky, H. W. *Chem. Vap. Deposition* **2001**, *7*, 105.

(2) (a) Cowley, A. H.; Jones, R. A. *Angew. Chem., Int. Ed. Engl.* **1989**, *28*, 1208. (b) Atwood, D. A.; Jones, R. A.; Cowley, A. H.; Bott, S. G.; Atwood, J. L. *J. Organomet. Chem.* **1992**, *434*, 143.

(3) (a) Cowley, A. H.; Jones, R. A. *Polyhedron* **1994**, *13*, 1149. (b) Fischer, R. A.; Miehr, A.; Ambacher, O.; Metzger, T.; Born, E. *J. Cryst. Growth* **1997**, *170*, 139. (c) Colombo, D. G.; Gilmer, D. C.; Young, V. G. J.; Campbell, S. A.; Gladfelter, W. L. *Adv. Mater.* **1998**, *10*, 220. (d) Horley, G. A.; O'Brien, P.; Park, J.-H.; White, A. J. P.; Williams, D. J. *J. Mater. Chem.* **1999**, *9*, 1289.

10.1021/ic034588x CCC: $25.00
Published on Web 08/28/2003

even to the preparation of nanomaterials such as group III−V whiskers, fibers, quantum dots, and pillared crystalline films.[4]

In recent years, the single molecular source concept as well as the related two-component CVD process has been applied to the design of new indium complexes containing chalcogenide elements such as oxygen and sulfur, since these are potentially useful for the preparation of In_2O_3 optical materials or In_2S_3 phases, which are used as transparent conductors in applications such as display panels and solar cell windows.[5] Deposition of In_2S_3 phases is best accomplished using precursors such as the dithiocarbamate complexes $In(S_2CNMeR)_3$ (R = Bu, hexyl) or thiocarboxylate and thiolate complexes,[6] while the preparation of In_2O_3 thin films has been achieved using the homoleptic β-diketonate complexes [In(acac)$_3$] and [In(tmhd)$_3$], tmhd = 2,2,6,6-tetramethylheptane-3,5-dionate, as well as the metal carboxylate [In{$O_2C(C_7H_{15})$}$_3$].[7] Among the common indium complexes such as the β-diketonates, carboxylates, and alkoxides, the alkoxides are the most versatile for tailoring chemical and physical properties at the molecular level. These rationally designed complexes have greatly simplified the process leading to successful fabrication of In_2O_3 thin films and the corresponding mixed oxide materials. We have adopted this strategy in the present study, by selecting a series of CF_3 substituted aminoalkoxide or ketoiminate ligands to stabilize the indium-containing complexes and make them suitable as source reagents for deposition of In_2O_3 thin films. The aminoalkoxide ligand is expected to exhibit behavior superior to that of the simple alkoxide ligand as the former would eliminate the necessity of introducing an extra donor group to stabilize the electron deficient group III alkoxide complexes.[8]

Experimental Section

General Information and Materials. Mass spectra were obtained on a JEOL SX-102A instrument operating in electron impact (EI) mode. ^{1}H, ^{13}C, and ^{19}F NMR spectra were recorded on Varian Mercury-400 or INOVA-500 instruments; chemical shifts are quoted with respect to tetramethylsilane for ^{1}H and ^{13}C NMR data and CF_3Cl for ^{19}F NMR data, respectively. The thermogravimetric analyses (TGA) were recorded on a Seiko TG/DTA 300 instrument under atmospheric pressure of N_2 with a flow rate of 100 sccm and with a heating rate of 10 °C/min. Elemental analyses were carried out at the NSC Regional Instrumentation Center at National Chiao Tung University, Hsinchu, Taiwan. All reactions were performed under an inert atmosphere using anhydrous solvents or solvents treated with appropriate drying reagent. The CF_3 substituted amino alcohol ligands of formulas $HOC(CF_3)_2CH_2NMe_2$ and $HOC(CF_3)_2CH_2NHR$, R = Me, CH_2CH_2OMe, and Bu^t, were prepared according to the literature method,[9] while the tridentate ketoimine ligand $O{=}C(CF_3)CH_2C(CF_3){=}NCH_2CH_2NMe_2$ was obtained from a reaction of hexafluoroacetylacetone with *N*,*N*-dimethyl-ethylenediamine in the presence of montmorillonite K10.[10]

The In_2O_3 thin films were characterized using scanning electron microscopy (SEM) on a Hitachi S-4000 system to study the surface morphology and by an X-ray diffractometer (XRD) with Cu Kα radiation. The resistivities were measured using a four-point probe method at room temperature, for which the instrument is assembled using a Keithley 2182 nanovoltmeter and a Keithley 2400 constant current source. The composition of the thin films was determined by X-ray photoelectron spectroscopy (XPS) utilizing a Physical Electronics PHI 1600 system with an Al/Mg dual anode X-ray source. The surface composition in atom percent was determined from the XPS spectra after 1−2 min sputtering with argon at 4 keV until a constant composition was obtained. Rutherford backscattering spectra (RBS) were acquired on a Van de Graaff accelerator (model KN-1008) using a 2−3 MeV $^4He^+$ beam. This instrument is installed at the Nuclear Science and Technology Development Center (NSTDC) of the National Tsing Hua University. The spectral data were then analyzed using the simulation program RUMP.[11]

Synthesis of 1. The amino alcohol ligand $HOC(CF_3)_2CH_2NHCH_2CH_2OMe$ (1.28 g, 5 mmol) was added dropwise into a diethyl ether solution (20 mL) of $InMe_3$ (0.8 g, 5 mmol) maintained at 0 °C, during which time a rapid evolution of methane was observed. The stirring was continued for 1 h to ensure the completion of the reaction. The solvent was then evaporated and the residue was subjected to sublimation at 130 °C/600 millitorr, giving a colorless material [$InMe_2(OC(CF_3)_2CH_2NHCH_2CH_2OMe)]_2$ (**1**) (1.04 g, 2.6 mmol), yield 52%. Single crystals of **1** suitable for X-ray diffraction study were obtained by recrystallization from a mixture of CH_2Cl_2 and hexane at room temperature.

Spectral data for **1** follow. MS (EI): *m*/*z* 384 {M^+ − Me}. ^{1}H NMR (400 MHz, $CDCl_3$, 298 K): δ 3.44 (t, 2H, CH_2O, $^3J_{HH}$ = 4.8 Hz), 3.33 (s, 3H, OMe), 2.93 (s, br, 2H, CH_2N), 2.83 (s, br, 2H, NCH_2), 2.11 (m, 1H, NH), −0.25 (s, 6H, InMe). ^{13}C NMR (100 MHz, $CDCl_3$, 298 K): δ 124.4 (q, CF_3, $^1J_{CF}$ = 290 Hz), 78.1 (m, $C(CF_3)_2$, $^2J_{CF}$ = 27.4 Hz), 69.7 (s, OMe), 58.7 (s, CH_2O), 49.7 (s, NCH_2), 48.8 (s, CH_2N), −5.3 (s, InMe). ^{19}F NMR (470 MHz, toluene-d_8, 298 K): δ −77.65 (s, br, CF_3). Anal. Calcd for $C_{18}H_{32}F_{12}In_2N_2O_4$: C, 27.09; H, 4.04; N, 3.51. Found: C, 27.07; H, 3.99; N, 3.36.

(4) (a) Dingman, S. D.; Rath, N. P.; Markowitz, P. D.; Gibbons, P. C.; Buhro, W. E. *Angew. Chem., Int. Ed.* **2000**, *39*, 1470. (b) Fischer, R. A.; Miehr, A.; Metzger, T.; Born, E.; Ambacher, O.; Angerer, H.; Dimitrov, R. *Chem. Mater.* **1996**, *8*, 1356. (c) Wohlfart, A.; Devi, A.; Maile, E.; Fischer, R. A. *Chem. Commun.* **2002**, 998. (d) Takahashi, N.; Niwa, A.; Takahashi, T.; Nakamura, T.; Yoshioka, M.; Momose, Y. *J. Mater. Chem.* **2002**, *12*, 1573.

(5) (a) Avaritsiotis, J. N.; Howson, R. P. *Thin Solid Films* **1980**, *80*, 63. (b) Minami, T.; Kumagai, H.; Kakumu, T.; Takata, S.; Ishii, M. *J. Vac. Sci. Technol., A* **1997**, *15*, 1069. (c) Wang, A.; Dai, J.; Cheng, J.; Chudzik, M. P.; Marks, T. J.; Chang, R. P. H.; Kannewurf, C. R. *Appl. Phys. Lett.* **1998**, *73*, 327. (d) Zhou, Z. B.; Cui, R. Q.; Pang, Q. J.; Wang, Y. D.; Meng, F. Y.; Sun, T. T.; Ding, Z. M.; Yu, X. B. *Appl. Surf. Sci.* **2001**, *172*, 245.

(6) (a) Shang, G.; Kunze, K.; Hampden-Smith, M. J.; Duesler, E. N. *Chem. Vap. Deposition* **1996**, *2*, 242. (b) O'Brien, P.; Otway, D. J.; Walsh, J. R. *Thin Solid Films* **1998**, *315*, 57. (c) Suh, S.; Hoffman, D. M. *Inorg. Chem.* **1998**, *37*, 5823. (d) Horley, G. A.; O'Brien, P.; Park, J.-H.; White, A. J. P.; Williams, D. J. *J. Mater. Chem.* **1999**, *9*, 1289.

(7) (a) Nomura, R.; Inazawa, S.; Matsuda, H.; Saeki, S. *Polyhedron* **1987**, *6*, 507. (b) Maruyama, T.; Fukui, K. *J. Appl. Phys.* **1991**, *70*, 3848. (c) Reich, S.; Suhr, H.; Waimer, B. *Thin Solid Films* **1990**, *189*, 293.

(8) (a) Schumann, H.; Frick, M.; Heymer, B.; Girgsdies, F. *J. Organomet. Chem.* **1996**, *512*, 117. (b) Miinea, L.; Suh, S.; Bott, S. G.; Liu, J.-R.; Chu, W.-K.; Hoffman, D. M. *J. Mater. Chem.* **1999**, *9*, 929. (c) Miinea, L. A.; Suh, S.; Hoffman, D. M. *Inorg. Chem.* **1999**, *38*, 4447. (d) Valet, M.; Hoffman, D. M. *Chem. Mater.* **2001**, *13*, 2135.

(9) (a) Chang, I.-S.; Willis, C. J. *Can. J. Chem.* **1977**, *55*, 2465. (b) Loeb, S. J.; Richardson, J. F.; Willis, C. J. *Inorg. Chem.* **1983**, *22*, 2736. (c) Chang, C.-H.; Hwang, K. C.; Liu, C.-S.; Chi, Y.; Carty, A. J.; Scoles, L.; Peng, S.-M.; Lee, G.-H.; Reedijk, J. *Angew. Chem., Int. Ed.* **2001**, *40*, 4651.

(10) Tung, Y.-L.; Tseng, W.-C.; Lee, C.-Y.; Chi, Y.; Peng, S.-M.; Lee, G.-H. *Organometallics* **1999**, *18*, 864.

(11) Thompson,M. O. *RUMP*, version 4.00 (beta); Computer Graphic Service, Ltd.: El Paso, TX, 2002.

Synthesis of 2. Procedures identical to that of **1** were followed, using amino alcohol ligand $HOC(CF_3)_2CH_2NHMe$ (0.21 g, 1 mmol) and trimethylindium (0.16 g, 1 mmol) dissolved in 20 mL of diethyl ether. Vacuum sublimation (120°C/420 millitorr) gave a colorless material $[InMe_2(OC(CF_3)_2CH_2NHMe)]_2$ (**2**, 0.22 g, 0.6 mmol) in 62% yield.

Spectral data for **2** follow. MS (EI) *m*/*z* 340 $\{M^+ - Me\}$. ^1H NMR (400 MHz, $CDCl_3$, 298 K): δ 2.91 (s, 2H, NCH_2), 2.41 (s, 3H, NMe), 1.59 (s, br, 1H, NH), −0.26 (s, 6H, InMe). ^{13}C NMR (100 MHz, $CDCl_3$, 298 K): δ 124.2 (q, CF_3, $^1J_{CF}$ = 288.6 Hz), 51.2 (s, NCH_2), 34.5 (s, NMe), −5.6 (s, InMe). ^{19}F NMR (470 MHz, toluene-d_8, 298 K): δ −75.11 (s, br, CF_3). Anal. Calcd for $C_{14}H_{24}F_{12}In_2N_2O_2$: C, 23.68; H, 3.41; N, 3.95. Found: C, 23.64; H, 3.47; N, 3.64.

Synthesis of 3. The procedure was identical to that of **1**, using amino alcohol $HOC(CF_3)_2CH_2NHBu^t$ (0.25 g, 1 mmol) and trimethylindium (0.16 g, 1 mmol) dissolved in 20 mL of diethyl ether. Sublimation at 110°C under a pressure of 550 millitorr gave a colorless material $[InMe_2(OC(CF_3)_2CH_2NHBu^t)]_2$ (**3**, 0.32 g, 0.8 mmol) in 80% yield.

Spectral data for **3** follow. MS (EI) *m*/*z* 382 $\{M^+ - Me\}$. ^1H NMR (400 MHz, $CDCl_3$, 298 K): δ 2.97 (d, 2H, NCH_2, $^3J_{HH}$ = 8.1 Hz), 1.46 (t, 1H, NH, $^3J_{HH}$ = 7.8 Hz), 1.19 (s, 9H, CMe_3), −0.11 (s, 6H, InMe). ^{13}C NMR (100 MHz, $CDCl_3$, 298 K): δ 124.4 (q, CF_3, $^1J_{CF}$ = 289.8 Hz), 78.5 (m, $C(CF_3)_2$, $^2J_{CF}$ = 27.5 Hz), 53.0 (s, NCH_2), 43.4 (s, CMe_3), 28.8 (s, CMe_3), −2.05 (s, InMe). ^{19}F NMR (470 MHz, toluene-d_8, 298 K): δ −75.91 (s, br, CF_3). Anal. Calcd for $C_{20}H_{36}F_{12}In_2N_2O_2$: C, 30.36; H, 4.48; N, 3.44. Found: C, 30.70; H, 4.56; N, 3.64.

Synthesis of 4. The procedure was identical to that of **1**, using the amino alcohol $HOC(CF_3)_2CH_2NMe_2$ (0.45 g, 2 mmol) and trimethylindium (0.32 g, 2 mmol) dissolved in 20 mL of diethyl ether. Sublimation at 110 °C under a pressure of 400 millitorr gave a white powder $[InMe_2(OC(CF_3)_2CH_2NMe_2)]_2$ (**4**, 0.61 g, 1.6 mmol) in 82% yield.

Spectral data for **4** follow. MS (EI) *m*/*z* 354 $\{M^+ - Me\}$. ^1H NMR (400 MHz, C_6D_6, 298 K): δ 2.39 (s, 2H, CH_2), 1.72 (s, 6H, NMe_2), 0.04 (s, 6H, InMe). ^{13}C NMR (100 MHz, C_6D_6, 298 K): 125.4 (q, CF_3, $^1J_{CF}$ = 290.8 Hz), 78.8 (m, $C(CF_3)_2$, $^2J_{CF}$ = 27.7 Hz), 58.3 (s, NCH_2), 47.6 (s, NMe_2), −4.5 (s, InMe). ^{19}F NMR (470 MHz, toluene-d_8, 298 K): δ −75.80 (s, CF_3). Anal. Calcd for $C_{16}H_{28}F_{12}In_2N_2O_2$: C, 26.04; H, 3.82; N, 3.80. Found: C, 25.70; H, 3.91; N, 3.75.

Synthesis of 5. The ketoimine ligand $O{=}C(CF_3)CH_2C(CF_3){=}NCH_2CH_2NMe_2$ (0.28 g, 1 mmol) was slowly added into a solution of trimethylindium (0.16 g, 1 mmol) in diethyl ether (15 mL) at 0 °C. Stirring of the solution was continued for 1 h, during which time the temperature was allowed to slowly increase to room temperature. The solvent was then evaporated, and the residue was subjected to sublimation at 80 °C/380 millitorr, giving colorless $[InMe_2(OC(CF_3){=}CHC(CF_3){=}NCH_2CH_2NMe_2)]$ (0.31 g, 0.73 mmol) in 74% yield. Single crystals of **5** suitable for X-ray diffraction study were obtained by repeated sublimation under a slightly higher pressure of 0.55 Torr at 70 °C.

Spectral data for **5** follow. MS (EI) *m*/*z* 407 $\{M^+ - Me\}$. ^1H NMR (400 MHz, C_6D_6, 298 K): δ 5.90 (s, 1H, CH), 3.09 (t, 2H, NCH_2, $^3J_{HH}$ = 5.4 Hz), 1.74 (t, 2H, NCH_2, $^3J_{HH}$ = 5.8 Hz), 1.45 (s, 6H, NMe_2), −0.11 (s, 6H, InMe). ^{13}C NMR (100 MHz, 298 K): δ 171.69 (q, $C(CF_3)$, $^2J_{CF}$ = 32.1 Hz), 160.77 (q, $C(CF_3)$, $^2J_{CF}$ = 26.4 Hz), 119.75 (q, CF_3, $^1J_{CF}$ = 284.2 Hz), 119.54 (q, CF_3, $^1J_{CF}$ = 286.7 Hz), 85.74 (s, CH), 57.93 (s, NCH_2), 46.43 (s, NCH_2), 44.32 (s, NMe_2), −7.12 (s, InMe). ^{19}F NMR (470 MHz, toluene-d_8, 298 K): δ −65.99 (s, CF_3), δ −75.74 (s, CF_3). Anal. Calcd for $C_{11}H_{17}F_6InN_2O$: C, 31.30; H, 4.06; N, 6.64. Found: C, 31.53; H, 4.11; N, 6.68.

Table 1. X-ray Structural Data of Complexes **1** and **5**

	1	**5**
formula	$C_{18}H_{32}F_{12}In_2N_2O_4$	$C_{11}H_{17}F_6InN_2O$
mol wt	798.10	422.09
T	293(2) K	173(2) K
cryst syst	monoclinic	monoclinic
space group	$P2_1/c$	$P2_1/n$
a (Å)	9.0999(4)	10.7743(6)
b (Å)	12.0148(5)	11.1724(6)
c (Å)	13.1052(4)	13.3760(7)
β (deg)	103.498(1)	99.179(1)
V (Å^3)	1393.26(11)	1589.51(15)
Z	2	4
D_c (g/cm^3)	1.902	1.764
μ(Mo Kα) mm^{-1}	1.762	1.547
F(000)	784	832
θ range	2.30−28.73°	2.26−28.73°
cryst size, mm^3	0.3 × 0.2 × 0.15	0.25 × 0.25 × 0.02
index ranges, *h*, *k*, *l*	−12 12, −15 16, −17 17	−14 14, −15 14, −18 17
reflns collected	16099	18452
indep reflns	3603 (R_{int} = 0.0279)	4105 (R_{int} = 0.0232)
data/restraints/params	3603/0/249	4105/0/327
GOF on F^2	0.966	1.017
R [$I > 2\sigma(I)$]	R1 = 0.0186, wR2 = 0.0427	R1 = 0.019, wR2 = 0.048
final R (all data)	R1 = 0.0266, wR2 = 0.0444	R1 = 0.029, wR2 = 0.051
D-map, max/min, e/Å^3	0.313/−0.531	0.438/−0.653

X-ray Crystallography. Single crystal X-ray diffraction data were measured on a Bruker SMART CCD diffractometer using λ(Mo Kα) radiation (λ = 0.71073 Å, $2\theta_{max} \leq 57.5°$, ω scan mode) and a graphite monochromator. The data collection was executed using the SMART program. Cell refinement and data reduction were accomplished using the SAINT program. The structure was solved using the SHELXTL/PC package and refined using full-matrix least-squares. An empirical absorption correction was applied with the SADABS routine (part of the SHELXTL program). The structure was solved by direct methods using the SHELXTL suite of programs. All non-hydrogen atoms were refined anisotropically by full-matrix least-squares on F^2. Hydrogen atoms were placed in calculated positions and allowed to ride on the parent atoms. Crystallographic refinement parameters of complexes **1** and **5** are summarized in Table 1, and the selected bond distances and angles of these complexes are listed in Tables 2−3, respectively.

CVD Procedures. The thermal CVD reactions were carried using a horizontal hot-wall reactor described elsewhere. The deposition chamber consisted of a 30 cm Pyrex tube with an internal diameter of 25 mm, placed within a Thermolyne 79300 tube furnace.[12] The Si(100) substrate was cleaned using the RCA cleaning method, for which the substrates were placed in dilute HF solution for 2 h, followed by washing with deionized water, and drying at 120°C for 10 min. The flow rate of O_2 carrier gas was adjusted to 5 sccm, and the deposition time was kept to 1−3 h. The actual deposition time was obtained by visually observing the complete consumption of the source compound.

Results and Discussion

Synthesis and Characterization. Trimethylindium readily reacts with the aminoalocohol ligands used in this study,

(12) (a) Lee, F.-J.; Chi, Y.; Hsu, P.-F.; Chou, T.-Y.; Liu, C.-S.; Peng, S.-M.; Lee, G.-H. *Chem. Vap. Deposition* **2001**, *7*, 99. (b) Liu, Y.-H.; Cheng, Y.-C.; Tung, Y.-L.; Chi, Y.; Chen, Y.-L.; Liu, C.-S.; Peng, S.-M.; Lee, G.-H. *J. Mater. Chem.* **2003**, *13*, 135.

Table 2. Selected Bond Distances (Å) and Angles (deg) of **1** (esd in Parentheses)

In(1)−C(5)	2.1397(14)	In(1)−C(6)	2.1408(14)
In(1)−O(1)	2.2034(8)	In(1)−N(1)	2.4655(10)
In(1)−O(1A)	2.3959(8)	O(1)−C(2)	1.3799(14)
C(1)−C(2)	1.5450(17)	N(1)−C(1)	1.4621(14)
N(1)−C(7)	1.4803(16)		
∠C(5)−In(1)−C(6)	143.72(6)	∠C(5)−In(1)−O(1)	110.94(5)
∠C(6)−In(1)−O(1)	105.19(5)	∠O(1A)−In(1)−N(1)	147.58(3)
∠O(1)−In(1)−N(1)	73.79(3)	∠C(5)−In(1)−N(1)	93.20(5)
∠C(6)−In(1)−N(1)	93.70(5)	∠C(5)−In(1)−O(1A)	97.47(5)
∠C(6)−In(1)−O(1A)	95.49(4)	∠O(1)−In(1)−O(1A)	73.81(3)
∠In(1)−O(1)−In(1A)	106.19(3)		

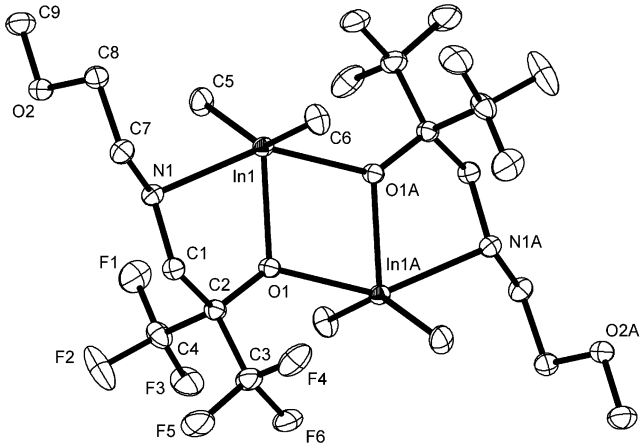

Figure 1. ORTEP drawing of complex **1** with thermal ellipsoids shown at the 30% probability level.

giving complexes with a proposed formula of $[InMe_2(OC(CF_3)_2CH_2NHR)]_2$, R = CH_2CH_2OMe (**1**), Me (**2**), and Bu^t (**3**), and $[InMe_2(OC(CF_3)_2CH_2NMe_2)]_2$ (**4**). In a typical synthesis, $InMe_3$ was first dissolved in diethyl ether solution, and to this solution was added a second diethyl ether solution containing the respective amino alcohol ligand in an equal amount. After the vigorous evolution of methane gas, a colorless precipitate was gradually formed which was collected and subjected to vacuum sublimation to give white products in yields of 52−82%. These compounds appear to be moderately air sensitive, as they give milky, insoluble materials upon dissolving in chlorinated solvents such as $CDCl_3$ for a period of 4−6 h. As a result, all NMR spectra were recorded using solutions freshly prepared within 5 min prior to the actual data collection, or simply using hydrocarbon solvents such as toluene-d_8.

The exact identity and molecular structure of **1** was determined by X-ray crystallography. Selected bond distances and angles are summarized in Table 2. As shown in Figure 1, the compound exhibits a dimeric molecular arrangement. The centrosymmetric, four-membered In_2O_2 ring which is common to this type of complex[13] is nearly planar, and each indium metal atom adopts a distorted trigonal bipyramidal geometry with two methyl groups in equatorial positions. The bridging alkoxide groups are located in both axial and equatorial positions, while the nitrogen atom of the aminoalkoxide group is in the axial position with the N−In−O bond angle to the opposite, axial alkoxide group being 147.58(3)°. Moreover, the equatorial In(1)−O(1) bond length of 2.2034(8) Å is significantly shorter than that to the axial alkoxide oxygen atom with In(1)−O(1A) distance = 2.3959(8) Å. The In(1)−N(1) distance of 2.466(1) Å which can be attributed to N→In dative bonding is slightly longer than the N→In interaction observed in the cyclic compound $Me_2In(C_6H_4CH_2NMe_2)$ (2.38(1) Å).[14] This bond length is also longer than the sum of the covalent radii of N(sp^3) and O (2.19 Å)[15] as well as the distance between the indium atom and the amide functional group observed in $MeIn[N(CH_2Ph)(2\text{-}NC_5H_4)]_2$ (2.146−2.169 Å).[16] Similar distorted trigonal bipyramidal geometry at the indium center has been noted in the closely related aluminum and gallium chiral aminoalkoxide complexes of the type $[Me_2MOR]_2$, where M = Al, R = $CHMeCH_2NMe_2$, $CHMeCH_2NH_2$; and M = Ga, R = $CHMeCH_2NMe_2$.[17] These structures are also dimeric in the solid state and consist of a central M_2O_2 rectangle and two five-membered heterocyclic rings located at each of the aluminum or gallium metal atoms.

After establishing the solid-state structures, the structural properties of complex **1** in solution were then explored. First, the ^{1}H NMR spectrum of **1** showed only a single set of In−Me resonance signals at δ −0.25 in $CDCl_3$ at room temperature. This observation is in contrast to the structure established by the single crystal X-ray analysis in the solid state, where two chemically nonequivalent In−Me groups were found, due to the asymmetric, coordinated $NHCH_2CH_2OMe$ pendant ligand attached to each of the In metal centers. For further investigation of the solution structures and fluxional behavior, we have concentrated on studies of variable temperature ^{1}H NMR spectra of the less complicated, NHMe derivative complex **2**.

First, we prepared a toluene-d_8 solution containing a 1:1 mixture of complexes **2** and **4**. Immediately after the solution was prepared, the ^{1}H NMR spectrum exhibited only one In−Me signal at δ 0.18, a position located between that of the parent complexes **2** (δ 0.15) and **4** (δ 0.19). Moreover, upon lowering the temperature to 213 K, the ^{1}H NMR spectrum gave at least six In−Me signals in the range δ 0.31−0.20, showing a complicated spectral pattern that was very different from that of the individual spectra of **2** and **4** observed under similar conditions. These findings obviously suggest the occurrence of rapid dimer to monomer dissociation, which then recombined to give three dimeric species in solution; one of them should possess the mixed structural character. This proposed dimer to monomer scrambling reaction is depicted in Scheme 1.

The VT ^{1}H NMR spectra of **2** were then recorded in d_8-toluene solution and are depicted in Figure 2. At 298 K, only one In−Me signal was observed which is in good agreement with that found for complex **1** in $CDCl_3$ solution under

(13) Veith, M.; Hill, S.; Huch, V. *Eur. J. Inorg. Chem.* **1999**, 1343.

(14) Khan, M.; Steevensz, R. C.; Tuck, D. G.; Noltes, J. G.; Corfield, P. W. R. *Inorg. Chem.* **1980**, *19*, 3407.

(15) Schumann, H.; Hartmann, U.; Wassermann, W.; Dietrich, A.; Goerlitz, F. H.; Ludwig, P.; Martin, H. *Chem. Ber.* **1990**, *123*, 2093.

(16) Zhou, Y.; Richeson, D. S. *Organometallics* **1995**, *14*, 3558.

(17) (a) Thiele, K.-H.; Hecht, E.; Gelbrich, T.; Duemichen, U. *J. Organomet. Chem.* **1997**, *540*, 89. (b) Hecht, E.; Gelbrich, T.; Thiele, K.-H.; Sieler, J. *Main Group Chem.* **2000**, *3*, 109.

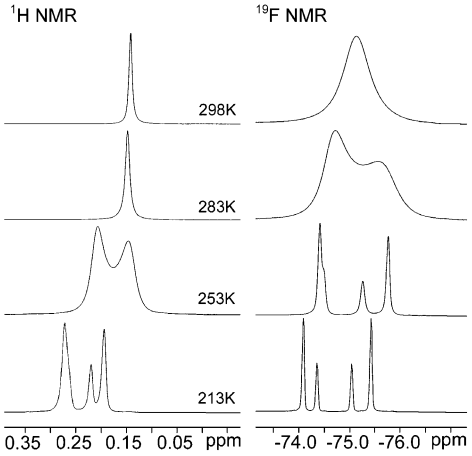

Figure 2. Variable temperature ^{1}H and ^{19}F NMR spectra of **2** in toluene-d_8, showing the regions of In−Me and CF_3 signals, respectively

Scheme 1

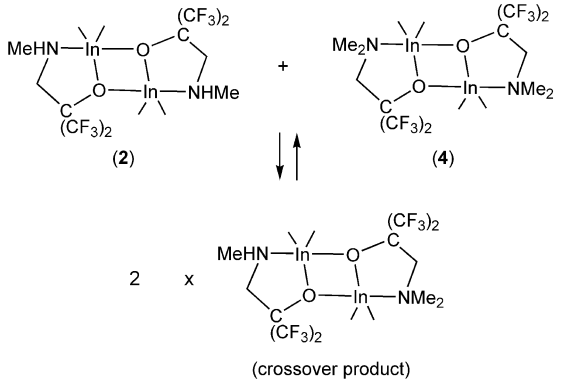

similar conditions. However, by gradually lowering the probe temperature to 253 K, the sharp singlet broadened and split into two overlapping signals located at δ 0.21 and 0.14. The unequal intensities of these resonances indicated that they are probably derived from two distinctive chemical species undergoing rapid interconversion in solution. Upon further lowering the temperature to 213 K, three distinct resonance signals become observable. The highest intensity signal at $\delta \sim 0.27$ consists of two overlapping signals, and their combined intensity match very well with those of the high field signals at δ 0.22 and 0.19, showing a ratio of approximately 1:2. We speculate that these signals belong to two interconvertible isomers that differ by virtue of the position of the methyl group on the NHMe fragment, which would afford two configurational isomers of the five-membered heterocyclic ring, namely *cis* and *trans* isomers (Scheme 2). The unequal intensities suggest that one isomer appears to be more stable than the other under the conditions examined. At higher temperatures, N→In bond cleavage would occur followed by rapid inversion of the configuration at the nitrogen atom, and regeneration of the N→In bond, allowing the occurrence of rapid *cis*−*trans* isomerization. Generally speaking, this isomerization is conceptually similar to the *cis*−*trans* equilibration observed in the dimer complexes $[Me_2MNMePh]_2$, M = Al, Ga, and In,[18] for which the interchangeable alkyl substituents are located at the central M_2N_2 rectangle, and are most likely to exchange via

Scheme 2

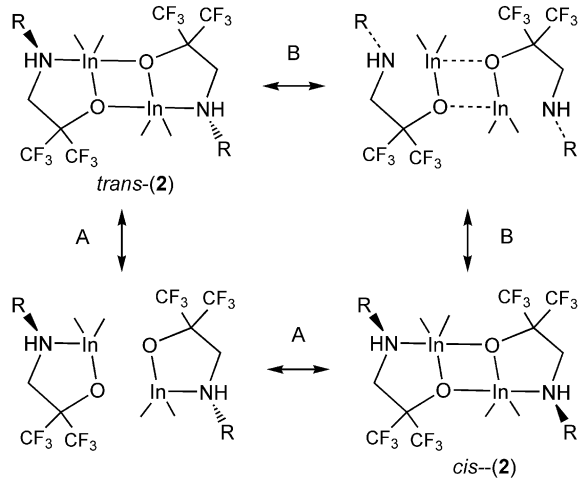

the dissociated monomers by a series of metal−nitrogen bond-breaking and forming reactions.

The variable temperature ^{19}F NMR spectra are also depicted in Figure 2, showing a similar pattern of fluxional behavior with four signals with an expected 2:1:1:2 pattern at the lowest temperature of 213 K and with only one broad signal at δ −75.1 at 298 K. These temperature-dependent spectra confirmed that the proposed isomerization is most likely caused by reversible dimer to monomer dissociation, followed by recombination (path A). This proposed pathway is supported by the detection of the crossover product upon mixing complexes **2** and **4** under a similar experimental condition. The second possibility (path B), which involves the prior dissociation of nitrogen from the indium atom, inversion at the nitrogen and reforming the inverted N→In bonding interaction, cannot be completely ruled out at this moment, as both reaction pathways are dissociative and may have very similar activation parameters. Finally, symmetrical NMe_2 substituted complex **4** failed to show any such behavior, undoubtedly due to its symmetrical nature which prevents formation of structurally distinct isomeric species in solution.

Following successful preparation of the described aminoalkoxide complexes **1**−**4**, we also treated the $InMe_3$ reagent with a different tridentate ketoimine ligand HOC(CF_3)=CH C(CF_3)=N$CH_2CH_2NMe_2$ in the hope of obtaining other types of source reagents, with physical characteristics more suitable for the CVD runs. This synthetic attempt afforded [$InMe_2$(OC(CF_3)=CHC(CF_3)=N$CH_2CH_2NMe_2$)] (**5**) (72% yield) as the only isolable product. Varying the experimental parameters such as reaction time, temperature, and solvent, or even by having an excess of ketoimine ligand, failed to produce any change in products. According to our ^{1}H NMR analysis, complex **5** possesses two chemically identical In−Me fragments appearing at high field (δ −0.11), while the rest of the proton resonance signals are clearly derived from one ligated ketoiminate fragment.

(18) (a) Beachley, O. T., Jr.; Bueno, C.; Churchill, M. R.; Hallock, R. B.; Simmons, R. G. *Inorg. Chem.* **1981**, *20*, 2423. (b) Park, J. T.; Kim, Y.; Kim, J.; Kim, K.; Kim, Y. *Organometallics* **1992**, *11*, 3320. (c) Styron, E. K.; Schauer, S. J.; Lake, C. H.; Watkins, C. L.; Krannich, L. K. *J. Organomet. Chem.* **1999**, *585*, 266.

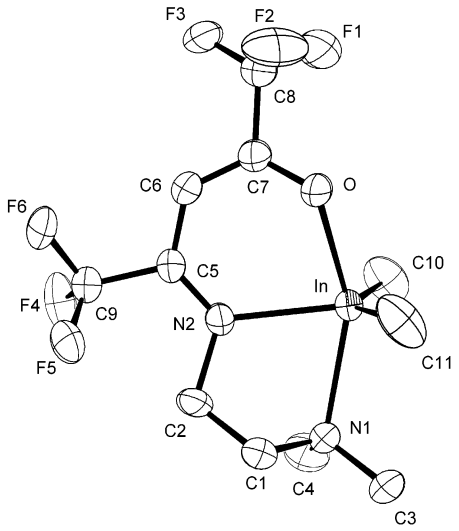

Figure 3. ORTEP drawing of complex **5** with thermal ellipsoids shown at the 50% probability level.

Table 3. Selected Bond Distances (Å) and Angles (deg) of **5** (esd in Parentheses)

In−O	2.251(3)	In−N(1)	2.428(2)
In−N(2)	2.321(2)	In−C(10)	2.141(2)
In−C(11)	2.142(2)	O−C(7)	1.315(4)
C(5)−C(6)	1.411(3)	C(6)−C(7)	1.351(3)
N(2)−C(5)	1.288(2)	N(2)−C(2)	1.553(9)
N(1)−C(1)	1.454(4)	C(1)−C(2)	1.486(10)
∠O−In−N(1)	153.3(1)	∠O−In−N(2)	80.4(1)
∠O−In−C(10)	100.4(1)	∠O−In−C(11)	86.9(1)
∠N(1)−In−N(2)	74.1(1)	∠N(1)−In−C(10)	96.1(1)
∠N(1)−In−C(11)	95.8(1)	∠C(10)−In−C(11)	135.9(1)
∠C(10)−In−N(2)	111.2(1)	∠C(11)−In−N(2)	112.9(1)

For further confirmation of the structure of **5**, a single crystal X-ray diffraction study was conducted, and the respective molecular structure is depicted in Figure 3, while selected interatomic distances and angles are collected in Table 3. The central indium atom has a distorted trigonal bipyramidal geometry, with two short bonds to the equatorial methyl carbon atoms (2.141−2.142 Å), and one long interaction to the N(1) atom that is located at the axial position (In−N(1) = 2.428(2) Å). The bond angle between the axial ligand fragments is consistent with significant deviation from linearity (∠O−In−N(1) = 153.3(1)°), which is due to the formation of two chelate rings within the molecule. Interestingly, the gross structure of **5** is akin to that of the gallium complex [$Me_2Ga(hfac)\cdot(NC_5H_5)$],[19] for which the pyridine ligand and one oxygen atom of the hfac ligand reside at the axial positions, showing a bond pattern that is in line with the ketoiminate fragment and NMe_2 terminus of the tridentate chelate ligand observed in **5**.

Thermal Analysis. The volatility and thermal stability of complexes **1**−**5** were investigated by thermogravimetric analysis (TGA) under an atmospheric pressure of N_2 (Figure 4). Generally speaking, the aminoalkoxide complexes **1**−**4** showed a similar pattern of weight loss, which generally began at the range of approximately 120 °C. The first $NHCH_2CH_2OMe$ derivative, **1**, seems to exhibit the lowest

(19) Beachley, O. T. J.; Gardinier, J. R.; Churchill, M. R.; Toomey, L. M. *Organometallics* **1998**, *17*, 1101.

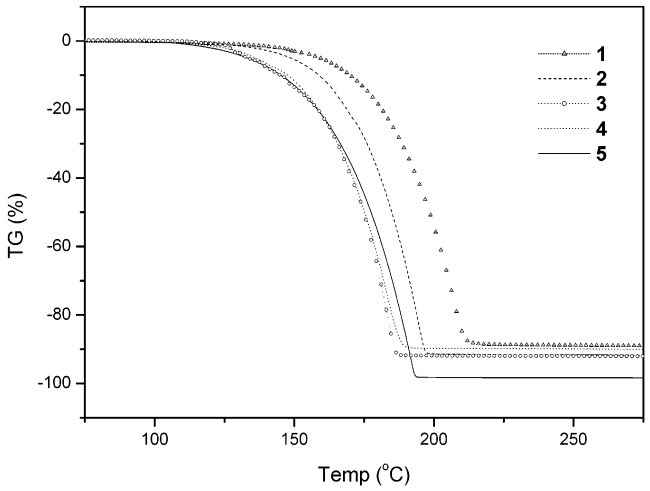

Figure 4. Thermogravimetric analysis (TGA) data of complexes **1**−**5**. All experiments were carried out at atmospheric pressure with N_2 as the carrier gas (100 sccm) and with a heating rate of 10 °C/min.

Table 4. Data Obtained from CVD Experiments Using Indium Complexes **2** and **5**[a]

entry (source compd)	gas (FR, sccm)	T_S (°C)	T_D (°C)	P_S (Torr)	thickness (Å)	O/In[b]	O/In[c]	C/In[b]
1 (**2**)	O_2 (5)	145	400	0.5	1100	0.7	1.4	0.08
2 (**2**)	O_2 (5)	145	450	0.5	1200	0.6	1.5	0.05
3 (**2**)	O_2 (5)	145	500	0.5	1000	0.8	1.8	0.07
4 (**5**)	O_2 (5)	80	400	0.5	750	1.1	1.5	0.06
5 (**5**)	O_2 (5)	80	450	0.5	1000	1.0	1.8	0.10

[a] T_S = source temperature, T_D = deposition temperature, P_S = system pressure, FR = flow rate. [b] atomic ratio measured from XPS data. [c] the data measured from RBS data.

volatility as its $T_{1/2}$ value, the temperature at which 50 wt % of the sample has been lost during TG analysis, is very close to 200 °C, which is the highest $T_{1/2}$ value ever observed within these series of compounds. In contrast, the three remaining compounds gave $T_{1/2}$ values in the range 175−185 °C, giving temperatures that are approximately 15−25 °C lower. This small difference in volatility can be traced to the MeO ether functional group present in complex **1**, versus the methyl or *tert*-butyl substituents utilized in other derivative complexes, which would considerably increase both the van del Waals interaction and the intermolecular N−H···O hydrogen bonding occurring between the N−H proton and the MeO ether linkage or even the alkoxy oxygen atom present in the sample,[20] and thus reduce the relative volatility. Moreover, the final residual weights are slightly higher (7.3−9.5 wt %), indicating a measurable amount of decomposition during heating. However, ketoiminate complex **5** appears to be much more robust to thermal decomposition, affording almost no residue (0.2 wt %) in the sample container upon heating to 300 °C. We speculate that its saturated five-coordinate environment is a main cause of the improved stability.

CVD Experiments. In order to study the usefulness of the as-prepared compounds in MOCVD applications, two

(20) (a) Chi, Y.; Hsu, P.-F.; Liu, C.-S.; Ching, W.-L.; Chou, T.-Y.; Carty, A. J.; Peng, S.-M.; Lee, G.-H.; Chuang, S.-H. *J. Mater. Chem.* **2002**, *12*, 3541. (b) Lai, Y.-H.; Chou, T.-Y.; Song, Y.-H.; Liu, C.-S.; Chi, Y.; Carty, A. J.; Peng, S.-M.; Lee, G.-H. *Chem. Mater.* **2003**, *15*, 2454.

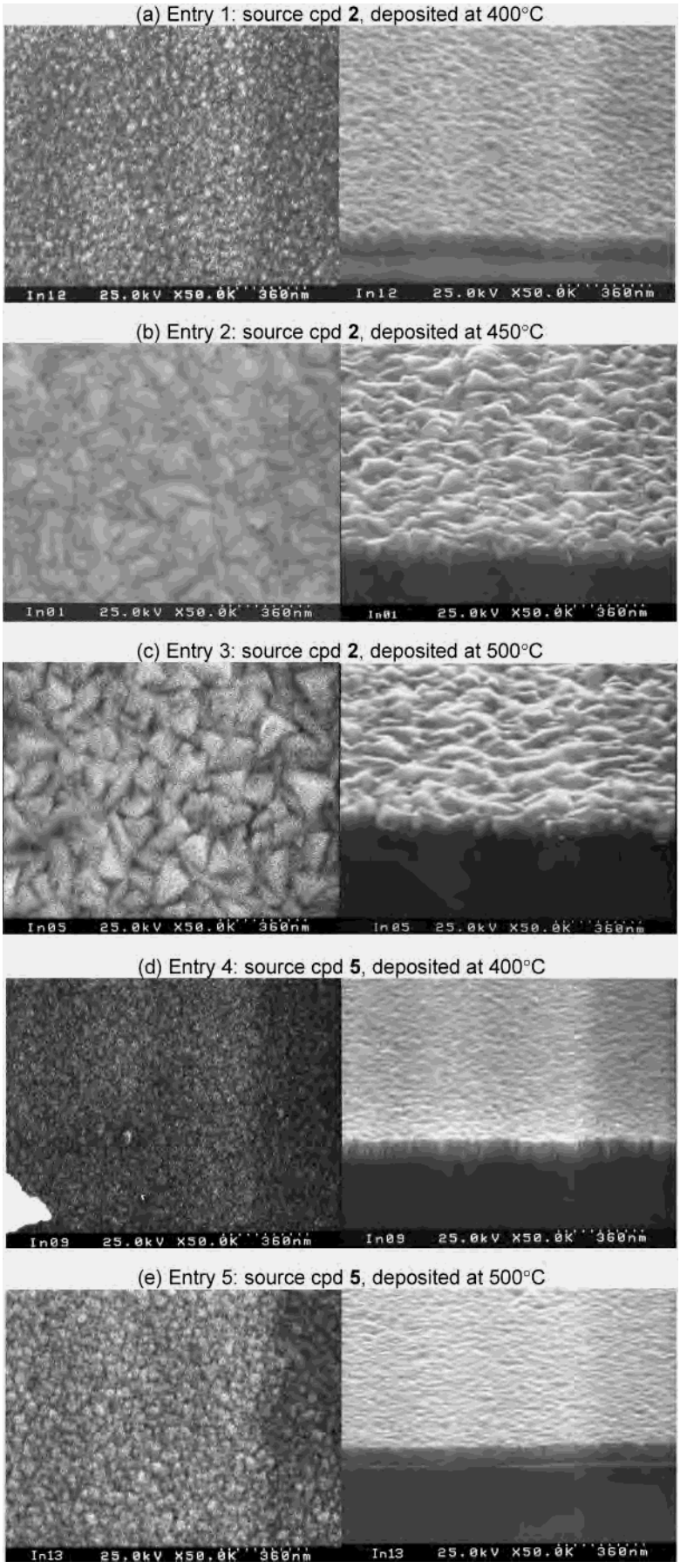

Figure 5. SEM micrographs of the as-deposited In_2O_3 thin films: (a) entry 1, (b) entry 2, (c) entry 3, (d) entry 4, and (e) entry 5; the top and 45° cross-sectional views are depicted at the left- and right-hand sides, respectively.

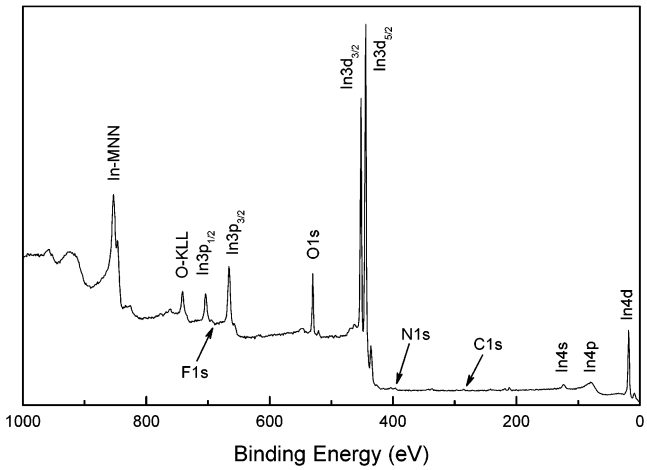

Figure 6. XPS spectra of In_2O_3 film deposited using **2** as CVD source reagent and at temperature $T_D = 450$ °C.

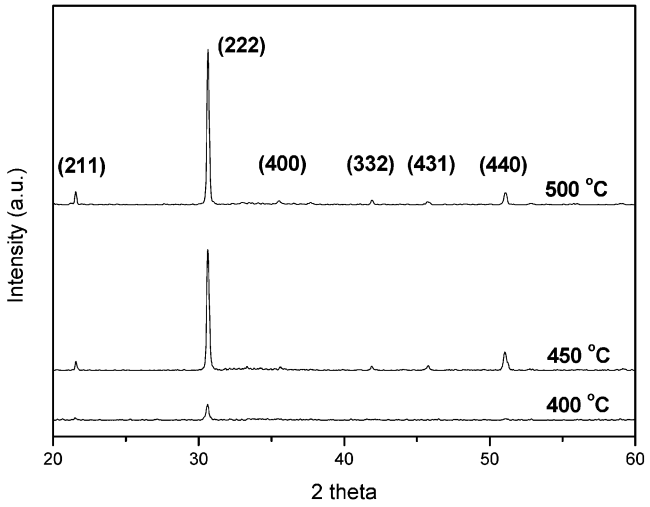

Figure 7. XRD pattern of the as-deposited In_2O_3 thin films deposited at various temperatures, for which complex **2** was employed as the source reagent.

representative examples **2** and **5** were tested for growing In_2O_3 in a conventional horizontal hot wall reactor. In a typical deposition process, O_2 was selected to convey the sample into the CVD chamber and to suppress the carbon content observed in the final In_2O_3 thin films. The sample reservoir was kept at 145 or 80 °C depending on the relatively volatility revealed by the TG analysis, while the growth temperature was maintained at temperatures of 400−500 °C with the system pressure being 300 millitorr. These parameters for the CVD runs are summarized in Table 4.

For complex **2**, the films obtained were light yellow and transparent at 400 °C and turned much darker at higher temperatures. All of the films adhered very well to the substrate (both Si wafer and quartz glass) as judged by the Scotch tape test. Their resistivity values ranged from 335 to 548 $\mu\Omega$ cm, which decreased with increasing deposition temperature. As indicated in Figure 5, the SEM images showed a thickness of ∼1100 Å, and the surface showed featureless morphology at 400 °C. Upon raising the temperatures to 450 and 500 °C, the surface turned much rougher, and the boundaries between each individual crystallite became clearly visible. The chemical binding state and thin film compositions were investigated by X-ray photoelectron spectroscopy (XPS). Before each experiment, the thin films were sputtered using Ar^+ ion to remove the surface contaminants. The C 1s peak observed at 284.5 eV was used to evaluate its atomic content present in the sample. The O 1s peak was assumed to be at ∼530.5 eV and together with the In $3d_{5/2}$ peak at ∼444.9 eV was used to gauge relative composition. The atomic compositions of the films were then calculated using sensitivity factors determined from the empirical peak area values and corrected for the system's transmission function.[21] The calculated O/In and C/In ratios are given in Table 4, respectively, while the contents of nitrogen (≤2 at. %) and fluorine (∼0 at. %) were not reported due to the low levels of these elements present in the as-deposited thin films. A typical XPS spectrum is depicted in Figure 6, showing the depleted oxygen atomic content and the possible locations of the carbon 1s peak at 284.5 eV, nitrogen 1s peak at 398.1 eV, and fluorine 1s peak at 684.9 eV. Moreover, it is important to note that it has been reported that the O/In ratio of the In_2O_3 stoichiometry cannot be reliably calculated because of preferential sputtering and sputtering induced decomposition which may cause the O/In ratio obtained by the XPS method to deviate significantly from the ideal value.[22] Our thin films were then subjected to Rutherford backscattering analysis (RBS) to obtain more the reliable O/In composition data, and these atomic percentages are listed in Table 4 for a direct comparison. It is noted that the calculated atomic ratios were now much closer to the expected composition of In_2O_3, except for the sample obtained at the highest temperature of 500 °C, confirming the formation of approximately In_2O_3 stoichiometry with minimum amount of oxygen deficiency with the as-deposited thin film materials.

Moreover, an X-ray diffraction (XRD) pattern for the film deposited at the lowest temperature of 400 °C shows only a weak signal at $2\theta = 30.58°$, which is due to the (222) diffraction of the cubic In_2O_3 phase (Figure 7), giving the first indication of the formation of a preferred (222) orientation. Upon further increasing the deposition temperature, the peak due to the (222) diffraction has gained its intensity, showing an increase of the preferred (222) alignment, while other less intense diffraction signals also appeared which provide supporting evidence for the characterization of In_2O_3 phase. Generally speaking, the polycrystalline In_2O_3 phase with a preferred orientation along the (222) planes is common; for example, O'Brien et al. have reported a similar XRD pattern of In_2O_3 thin film deposited using the dimeric source reagent $[Me_2In(acac)_2]_2$.[23] In contrast, Hoffman and co-workers were able to prepare the fluorine-doped In_2O_3 thin film material using alkoxide complex $In(OCMe(CF_3)_2)_3(H_2N\text{-}t\text{-}Bu)$,[24] where the similar

(21) Wagner, C. D.; Davis, L. E.; Zeller, M. V.; Taylor, J. A.; Raymond, R. H.; Gale, L. H. *Surf. Interface Anal.* **1981**, *3*, 211.

(22) Jeong, J. I.; Moon, J. H.; Hong, J. H.; Kang, J.-S.; Fukuda, Y.; Lee, Y. P. *J. Vac. Sci. Technol., A* **1996**, *14*, 293.

(23) Park, J.-H.; Horley, G. A.; O'Brien, P.; Jones, A. C.; Motevalli, M. *J. Mater. Chem.* **2001**, *11*, 2346.

(100) preferred orientation was also observed by deliberately increasing the fluorine content in the thin film samples,[25] compared with a more randomly distributed orientation.

The In_2O_3 thin film preparation was also extended to studies using the more volatile ketoiminate complex **5**. Basically, identical experimental parameters were employed for the deposition experiment, except that the reservoir temperature was lowered from 145 to 80 °C. Under these circumstances, a reduced amount of complex **5** enters into the CVD chamber so that the growth of In_2O_3 can be easily controlled giving a much smoother surface morphology (Figure 5). All physical characteristics such as the content and level of impurity and the XRD patterns are very similar to those from films deposited using complex **2** as the source reagent. These experimental observations suggest that although the ketoiminate ligand is a tridentate ligand and should be bound more strongly to the central In atom versus that of the bidentate aminoalkoxide ligand, both source reagents gave In_2O_3 films of similar quality, and their nitrogen and fluorine impurity contents are within the detection limits of our analytical instruments. This observation also implies that the O_2 co-reagent is very reactive and effective in terms of removal of ligated hydrocarbons, irrespective of their bonding mode.

Conclusions

A series of dimethyl aminoalkoxide indium complexes **1**−**4** and ketoiminate complex **5** were prepared and characterized by various spectroscopic and physical techniques. For the aminoalkoxide complexes with secondary amino substituents, VT NMR studies showed that they underwent rapid interconversion via both reversible dimer to monomer dissociation and the sequential rupture and reforming of N→In dative bond, giving a pair of *cis* and *trans* isomers in solution. Moreover, deposition of cubic In_2O_3 by MOCVD is possible using these newly prepared source reagents **2** and **5**, utilizing pure O_2 as the reactive carrier gas. We believe that these new CVD sources investigated would be superior to their parent source reagent $InMe_3$, due to the enhanced reactivity toward O_2 as well as the nonpyrophoric nature upon exposure to moistened air. For comparison, it was reported that $InMe_3$ would not produce the In_2O_3 films using a thermal low-pressure CVD process,[26] whereas the In_2O_3 films for use as plasma filters in thermal photovoltaic cells were successfully deposited using $InMe_3$ and oxygen as the reactant gas via atmospheric pressure chemical vapor deposition (APCVD).[27] Furthermore, the as-deposited thin films of our studies are oriented in the (222) direction, while the low level of nitrogen and fluorine contaminations confirms the effective elimination of both aminoalkoxide and ketoiminate ligands, although they have a greater tendency to produce stable metal chelate interaction. Our future directions will be focused at the preparation of indium-containing mixed-metal complexes and deposition of the mixed-metal oxide phases at lower temperatures.

Acknowledgment. Y.C. thanks the National Science Council and the Ministry of Education for financial support (NSC 91-2113-M-007-006) and (MOE program 89-FA04-AA).

Supporting Information Available: X-ray crystallographic file (CIF) for complexes **1** and **5**. This material is available free of charge via the Internet at http://pubs.acs.org.

IC034588X

(24) Miinea, L. A.; Hoffman, D. M. *J. Mater. Chem.* **2000**, *10*, 2392.
(25) (a) Maruyama, T.; Fukui, K. *Jpn. J. Appl. Phys.* **1990**, *29*, L1705. (b) Maruyama, T.; Fukui, K. *Thin Solid Films* **1991**, *203*, 297.
(26) Maruyama, T.; Kitamura, T. *Jpn. J. Appl. Phys.* **1989**, *28*, L1096.
(27) Murthy, S. D.; Langlois, E.; Bhat, I.; Gutmann, R.; Brown, E.; Dzeindziel, R.; Freeman, M.; Choudhury, N. *AIP Conf. Proc.* **1996**, *358*, 290.